

THE CONTRIBUTION OF PARTICLE IMPACT TO THE PRODUCTION OF Fe K α EMISSION FROM ACCRETING BLACK HOLES

D. R. BALLANTYNE

Canadian Institute for Theoretical Astrophysics, McLennan Laboratories, 60 St. George Street, Toronto, ON M5S 3H8, Canada;
ballantyne@cita.utoronto.ca

AND

A. C. FABIAN

Institute of Astronomy, University of Cambridge, Cambridge CB3 0HA, UK

Received 2003 February 14; accepted 2003 April 10

ABSTRACT

The iron K α line is perhaps the most important spectral diagnostic available in the study of accreting black holes. The line is thought to result from the reprocessing of external X-rays by the surface of the accretion disk. However, as is observed in the solar corona, illumination by energetic particles may also produce line emission. In principle, such a process may be uncorrelated with the observed X-rays and could explain some of the unexpected variability behavior of the Fe K α line. This paper compares predictions of iron K α flux generated by impacting electrons and protons to that from photoionization. Nonthermal power laws of electrons are considered as well as thermal distributions of electrons and virialized protons. The electrons are thought to originate in a magnetically dominated accretion disk corona, while the protons are considered in the context of a two-phase (hot/cold) accretion scenario. In each case, the Fe K α flux from particle impact is found to be less than 1% of that produced by photoionization by a hard X-ray power law (normalized to the same energy flux as the particles). Thus, the electrons or protons must strike the disk with 10^2 – 10^4 times more energy flux than radiation for particle impact to be a significant producer of Fe K α flux. This situation is difficult to reconcile with the observations of hard X-ray spectra or the proposed particle acceleration mechanisms in the accretion disk corona. Truncated accretion flows must be externally illuminated by hard X-rays in order to produce the Fe K α line, as proton impact is very inefficient in generating line emission. In contrast to the Sun, our conclusion is that, with the possible exception for localized regions around magnetic footpoints, particle impact will not be an important contributor to the X-ray emission in accreting black holes.

Subject headings: accretion, accretion disks — black hole physics — line: formation — radiation mechanisms: nonthermal — X-rays: general

1. INTRODUCTION

An iron K α emission line at 6.4 keV is commonly observed in the X-ray spectra of active galactic nuclei (AGNs) and Galactic black hole candidates (GBHCs). The equivalent widths of the lines are usually ~ 100 – 300 eV (Mushotzky, Done, & Pounds 1993; Nandra et al. 1997; Reeves & Turner 2000), suggesting that a significant column of iron is necessary to produce the required emission. This was confirmed with the discovery of the Compton reflection hump between 20 and 30 keV (Pounds et al. 1990; Nandra & Pounds 1994), which is a natural outcome of X-ray reprocessing in optically thick material (Lightman & White 1988; Guilbert & Rees 1988). In some cases, sensitive observations of the Fe K α line have found them to possess broad low-energy wings, consistent with the profile expected from a spinning accretion disk close to the black hole (see the reviews by Fabian et al. 2000 and Reynolds & Nowak 2003). These relativistically broadened lines have been seen in both AGNs (e.g., Tanaka et al. 1995; Nandra et al. 1997, 1999; Fabian et al. 2002) and GBHCs (e.g., Martocchia et al. 2002; Miller et al. 2002a, 2002b, 2002c) and provide strong evidence that the optically thick reflector responsible for the shape of the X-ray continuum is the inner region of the accretion disk. Thus, there has been considerable attention paid in recent years to the Fe K α line and X-ray

reflection features in accreting black holes, as they may probe the physics of the flows only a few Schwarzschild radii from the event horizon.

The phenomenology outlined above has given rise to a theoretical framework in which the X-rays are generated by some process in a corona above the accretion disk (Galeev, Rosner, & Vaiana 1979; Haardt & Maraschi 1991, 1993; Haardt, Maraschi, & Ghisellini 1994). Roughly half of the X-ray power illuminates the disk, is reprocessed, and then reemitted as a reflection spectrum that carries the Fe K α line and reflection hump (George & Fabian 1991; Matt, Perola, & Piro 1991). The iron line is produced by fluorescence; that is, incoming X-rays (usually in the form of a power law) with energies greater than 7.1 keV can remove a K shell electron from an iron atom or ion. The excited ion can then relax by a radiative transition into the K shell, or by the expulsion of an outer shell electron (the nonradiative Auger effect). With this mechanism the flux in the line is directly proportional to the ionizing flux (Basko 1978; Bai 1979), so that changes in the illuminating continuum should give rise to correlated changes in the Fe line flux. However, long monitoring campaigns of certain bright AGNs have shown that, at least in those sources, the Fe K α line exhibits weak variability on short timescales despite large changes in the continuum (e.g., Chiang et al. 2000; Reynolds 2000; Vaughan & Edelson 2001). Revisions to the standard

disk-corona model are necessary to explain this behavior (Reynolds 2001; Fabian & Vaughan 2003; Ballantyne, Vaughan, & Fabian 2003).

Fluorescence from photoionization is not the only mechanism able to generate an iron K line. Electron bombardment of the accretion disk can also produce line emission from iron if the kinetic energy of the particle is greater than 7.1 keV. This process has been used to explain enhanced line emission from the Sun (e.g., Zarro, Dennis, & Slater 1992), where electrons energized in the solar corona travel down magnetic field lines and strike the photosphere (Dennis & Schwartz 1989). As accretion disks likely also possess such magnetized coronae (Merloni & Fabian 2001), it is possible that similar situations would arise and result in Fe K α emission by electron bombardment.

In accretion disk coronae there exists a bath of thermal electrons with temperature $kT \approx 100\text{--}200$ keV (which generates the primary X-ray power law through Comptonization of the disk UV photons). There may also be a non-negligible amount of nonthermal electrons present in the corona. Evidence for these particles has been found in *Compton Gamma Ray Observatory* observations of Cyg X-1 in its soft state (Gierliński et al. 1999) and GRS 1915+105 (Zdziarski et al. 2001). These data, when combined with simultaneous hard X-ray observations, show that the X-ray power law extends to energies greater than 600 keV. Such spectra can be well fitted by a model of Comptonization in a hybrid thermal/nonthermal plasma (Coppi 1999). At present, there are no analogous observations for radio-quiet AGNs, but it is expected that the disk-corona physics will be similar for the two systems.

Proton illumination will also produce Fe K α emission in a manner analogous to electron bombardment. This may occur in a geometry where the optically thick accretion disk is disrupted into a hot ion flow close to the black hole (e.g., Meyer & Meyer-Hofmeister 1994; Róžańska & Czerny 2000a; Manmoto et al. 2000; Manmoto & Kato 2000; Meyer, Liu, & Meyer-Hofmeister 2000; Spruit & Deufel 2002). This configuration may be relevant to GBHCs in the low/hard state (Esin, McClintock, & Narayan 1997; Done & Życki 1999; Barrio, Done, & Nayakshin 2003) and low-luminosity AGNs (e.g., Quataert et al. 1999). In this scenario, the accretion energy is envisaged to be dissipated into the protons within the central optically thin flow, which then rapidly reach the virial temperature as they can be thermally decoupled from the electrons (Shapiro, Lightman, & Eardley 1976). The majority of the accretion energy is carried into (or advected) into the black hole by the protons with little or no observational signatures. Thus, these “advection-dominated accretion flows” (ADAFs) can be very radiatively inefficient (Ichimaru 1977; Rees et al. 1982; Narayan & Yi 1994). However, if the optically thick disk partially overlaps with the ADAF (for example, in the region where evaporation of the disk is taking place), then the hot protons in the ADAF will interact with the disk, significantly heating its surface (Spruit & Haardt 2000; Deufel & Spruit 2000; Deufel, Dullemond, & Spruit 2002) and possibly producing Fe K α emission. Proton impact ionization would also be relevant if a two-temperature corona exists above an untruncated accretion disk (Di Matteo, Blackman, & Fabian 1997).

If energetic coronal electrons (in an accretion disk-corona model) or virialized protons (in a truncated disk-ADAF model) strike the accretion disk, they would produce Fe K α

emission. If this process is sufficiently efficient, it could generate an observable line that is not strongly correlated with the continuum (e.g., Petrucci et al. 2002). This paper considers Fe K α production from particle impact onto accretion disks and compares it with the more traditional mechanism of photoionization. We consider incident beams consisting of thermal or nonthermal electrons and virialized protons. The goal is to evaluate under which circumstances, if any, particle bombardment will be an important contributor to the Fe K α line. The theory needed to calculate the expected line flux is outlined in § 2, and § 3 presents the results. In § 4 we consider the implications of the computations on particle acceleration mechanisms and the two different models of accretion geometry. A summary and our conclusions are presented in § 5.

2. MECHANISMS OF Fe K α PRODUCTION

2.1. Electron Bombardment

Consider a beam of electrons incident on the normal of an accretion disk with a spectral flux of \mathcal{N}_E electrons $\text{cm}^{-2} \text{s}^{-1} \text{keV}^{-1}$ at kinetic energy E . In both AGNs and GBHCs, the disk is hot enough so that both hydrogen and helium are fully ionized. Therefore, each incident electron will lose energy by Coulomb interactions with the hydrogen ions as it travels through the disk (Emslie 1978):

$$\frac{dE}{dt} = -2\pi e^4 \Lambda \frac{nv}{E}, \quad (1)$$

where e is the electron charge in esu, and n , v , and E are the instantaneous total hydrogen number density, electron velocity, and energy, respectively. Λ is the Coulomb logarithm

$$\Lambda = \ln\left(\frac{Eb_0}{e^2}\right), \quad (2)$$

where b_0 is the maximum impact parameter for the scattering event. Equation (1) differs from the classic analysis by Spitzer (1962) by ignoring the correction owing to thermal motion of the target electrons (Emslie 1978). This “cold target” approximation holds if $E \gg kT$, where T is the electron temperature of the accretion disk. Since we are interested in incoming electrons with $E > \chi$, where $\chi = 7.112$ keV is the ionization potential for neutral iron, this condition will hold for both AGN ($kT \sim 10$ eV) and GBHC ($kT \sim 500$ eV) disks.

As each incident electron decelerates¹ from its initial energy E_0 , it can eject a K shell electron from iron as long as its energy remains above χ . Thus, the resulting Fe K α line flux in photons $\text{cm}^{-2} \text{s}^{-1}$ is (e.g., Emslie, Phillips, & Dennis 1986; see the Appendix)

$$\mathcal{F}_{\text{ei}} = \frac{1}{2}\beta\omega \int_0^\infty \mathcal{N}_E(E_0) \left[\int_{E=E_0}^{E=\chi} \sigma_{\text{ei}}(E) n_{\text{Fe}} v(E) dt \right] dE_0, \quad (3)$$

where ω is the K fluorescence yield of iron, β is the K α to K β branching ratio, σ_{ei} is the K-shell ionization cross

¹ About 10^{-5} of the energy lost by the electron through scattering is radiated away as bremsstrahlung emission in the X-ray band, with the remainder ending up as heat (see, e.g., Tatischeff 2002). This radiation is ignored here.

section of iron owing to electron impact, and n_{Fe} is the number density of iron atoms. The inner integral in the above equation counts the number of Fe K α photons produced by an electron with initial energy E_0 as it loses energy passing through the disk. This then must be integrated over the distribution of initial electron energies to find the total Fe K α line flux. The factor of $\frac{1}{2}$ in front of the expression accounts for the fact that roughly half of the K α photons produced will be emitted away from the disk surface. We assume here, and in the treatment for photoionization described below, that all of the line photons emitted toward the surface escape to infinity.

Equation (1) can be used to rewrite the above expression in a more useful form:

$$\mathcal{F}_{\text{ei}} = \frac{1}{2} \frac{\beta \omega A_{\text{Fe}}}{2\pi e^4 \Lambda} \int_{\chi}^{\infty} \mathcal{N}_E(E_0) \left[\int_{\chi}^{E_0} \sigma_{\text{ei}}(E) E dE \right] dE_0, \quad (4)$$

where A_{Fe} is the abundance of iron relative to hydrogen in the disk, and we have changed the lower limit of the outer integral to the iron K-shell ionization energy (lower energies cannot produce K α lines). Note that this expression is independent of the density distribution of the target.

Of course, electrons with larger energies travel a greater distance before their kinetic energy falls below χ . Emslie (1978) showed that an electron with initial energy E_0 will have an energy $E = E_0(1 - 6\pi e^4 \Lambda N_{\text{H}}/E_0^2)^{1/3}$ after traversing a hydrogen column N_{H} . Therefore, the minimum initial energy needed by an electron to just be able to K-shell ionize an iron atom after passing through a column N_{H} is the solution of

$$E_{\text{min}}^3 - 6\pi e^4 \Lambda N_{\text{H}} E_{\text{min}} - \chi^3 = 0. \quad (5)$$

Using this relation to replace the infinity in the outer integral of equation (4), will allow us to calculate \mathcal{F}_{ei} as a function of N_{H} into the accretion disk.

2.2. Proton Bombardment

If protons are the incident particles then the equation for the energy loss rate is modified only² by a factor of m_p/m_e (Emslie 1978):

$$\frac{dE}{dt} = -2\pi e^4 \frac{m_p}{m_e} \Lambda \frac{nv}{E}, \quad (6)$$

where m_p is the proton mass, m_e is the electron mass, and now E is the kinetic energy of the impacting proton. Note that protons lose their energy much more rapidly than electrons. As before, we have assumed the cold target approximation which in this case requires $E \gg (m_p/m_e)kT$. For AGN disks, this condition implies $E \gg 18$ keV, while it is $E \gg 900$ keV for the hotter GBHC disks. The virial temperature for a proton a distance r away from a black hole is $kT_{\text{vir}} = 156(r/R_S)^{-1}$ MeV, where $R_S = 2GM/c^2$ is the Schwarzschild radius for a black hole of mass M . Therefore, assuming the protons in the ADAF reach the virial temperature, their energies will be greater than 1 MeV if $r < 100 R_S$, and so equation (6) will be valid for both AGNs and GBHCs.

² Strictly speaking, Λ is a function of the reduced mass of the scattering interaction and so will change with the different incident particle. However, the dependence is logarithmic in nature and so can safely be neglected.

We can now write down the analogous expression to equation (4) for the Fe K α line flux due to proton impact (see the Appendix):

$$\mathcal{F}_{\text{pi}} = \frac{1}{2} \frac{\beta \omega A_{\text{Fe}}}{2\pi e^4 \Lambda} \frac{m_e}{m_p} \int_{\chi}^{\infty} \mathcal{P}_E(E_0) \left[\int_{\chi}^{E_0} \sigma_{\text{pi}}(E) E dE \right] dE_0, \quad (7)$$

where \mathcal{P}_E is the spectral proton flux (protons $\text{cm}^{-2} \text{s}^{-1} \text{keV}^{-1}$) normally incident on the disk, and $\sigma_{\text{pi}}(E)$ is the K-shell ionization cross section of iron due to a proton with kinetic energy E . This expression differs notably from equation (4) by a factor of m_e/m_p ; therefore, unless this is compensated by the cross section, protons will be a much less significant producer of Fe K α photons than electrons.

After passing through a column N_{H} , a proton with initial energy E_0 will have an energy (Emslie 1978)

$$E = E_0 \left[1 - 4\pi e^4 \Lambda \left(\frac{m_p}{m_e} \right) \frac{N_{\text{H}}}{E_0^2} \right]^{1/2}. \quad (8)$$

Therefore, as with the electrons (eq. [5]), we can calculate the minimum kinetic energy a proton must have to just be able to ionize iron at the bottom of a column N_{H} :

$$E_{\text{min}} = \sqrt{\chi^2 + 4\pi e^4 \Lambda (m_p/m_e) N_{\text{H}}}. \quad (9)$$

Replacing the infinity with $E_{\text{min}}(N_{\text{H}})$ in the outer integral in equation (7) gives the total Fe K α flux produced through a column N_{H} .

2.3. Photoionization

There are many previous studies that have computed the Fe K α fluxes expected from photoionization (Hatchett & Weaver 1977; Basko 1978, 1979; Bai 1979). In this work, however, we will use the simplest expression for the line flux:

$$\mathcal{F}_{\text{photo}} = \frac{1}{2} N_{\text{H}} A_{\text{Fe}} \omega \beta \int_{\chi}^{\infty} F_{\epsilon}(\epsilon) \sigma_{\text{photo}}(\epsilon) d\epsilon, \quad (10)$$

where $F_{\epsilon}(\epsilon)$ is the photon flux (photons $\text{cm}^{-2} \text{s}^{-1} \text{keV}^{-1}$) incident on the normal of the accretion disk at energy ϵ , and σ_{photo} is the K-shell photoionization cross section of iron. As in the expression for electron impact production of Fe K α (eq. [4]), this equation assumes that iron is the only metal in the gas. Furthermore, equation (10) is only valid in the optically thin limit. That is, we are ignoring any attenuation of the incident X-rays or the outgoing Fe K α line photons. Therefore, we are limited to columns $N_{\text{H}} \leq 1/(1.2\sigma_{\text{T}}) = 1.25 \times 10^{24} \text{cm}^{-2}$, where σ_{T} is the Thomson cross section, and we have assumed a 10% abundance of helium (by number). The implications of limiting the calculations to Thomson thin columns are considered in the next section.

2.4. Charge Exchange

Another particle process that can produce Fe K α emission is charge exchange collisions. These are reactions of the following form: $\text{Fe}^{q+} + \text{A} \rightarrow \text{Fe}^{(q-1)+} + \text{A}^+$, where ‘‘A’’ is usually H, H₂, or He. The product Fe ion is often left in an excited state and will produce line emission as it relaxes. This collision differs from those described above in that the Fe ion is the energetic particle and the hydrogen or helium atom is the target. This process may be important for explaining the strong and broad K α lines from hydrogenic

and helium-like Fe observed in the Galactic ridge X-ray emission (Tanaka, Miyaji, & Hasinger 1999; Tanaka 2002). In this case, highly ionized Fe ions in the cosmic-ray distribution interacting with neutral Galactic gas would produce the needed line emission.

For the accretion disk scenario that is considered here, it is unlikely that charge exchange will be an important process, as there are very few neutral H and He atoms available for the reaction. Other metal ions could act as donors in a collision with Fe, but for typical cosmic abundances, encounters with the correct kinematics would be extremely rare. However, charge exchange may possibly be relevant to iron K lines emitted from the molecular torus of AGN unification schemes (e.g., Ghisellini, Haardt, & Matt 1994; Krolik, Madau, & Zycki 1994) if there is a flux of energetic Fe ions incident on this gas.

3. RESULTS

3.1. Electron Impact Versus Photoionization

To determine how efficient electron impact is in producing an Fe $K\alpha$ line in comparison to photoionization, we calculate the ratio of equations (4) and (10):

$$\frac{\mathcal{F}_{\text{ei}}}{\mathcal{F}_{\text{photo}}} = \frac{\int_{\chi}^{E_{\text{min}}(N_{\text{H}})} \mathcal{N}_E(E_0) \left[\int_{\chi}^{E_0} \sigma_{\text{ei}}(E) E dE \right] dE_0}{2\pi e^4 \Lambda N_{\text{H}} \int_{\chi}^{\infty} F_{\epsilon}(\epsilon) \sigma_{\text{photo}}(\epsilon) d\epsilon}. \quad (11)$$

Considering this ratio will also help negate the effects of absorption and scattering on the $K\alpha$ line that were ignored in the individual expressions. This value will nevertheless be only an upper limit, because in the true Thomson thick case high-energy photons can scatter down to energies where they can ionize iron and produce a $K\alpha$ photon. Some fraction of the line photons will escape the layer, but to accurately treat this process requires a numerical prescription.

The K-shell photoionization cross section (σ_{photo}) was taken from the tabulation by Verner & Yakovlev (1995). The empirical fit formula of Hombourger (1998) was used to compute the cross section for K-shell ionization by electron impact.³ These cross sections are plotted between χ and 200 keV in Figure 1, where the x -axis is used for both photon energy and electron kinetic energy. The cross section σ_{photo} is roughly proportional to ϵ^{-3} and thus falls off much more rapidly than σ_{ei} ; however, σ_{photo} is significantly greater than σ_{ei} for energies below 40 keV.

A power-law photon spectrum was assumed for all the calculations described below: $F_{\epsilon}(\epsilon) = F_0(\epsilon/\chi)^{-\Gamma}$, where $\Gamma = 1.7, 1.8, 1.9, \text{ or } 2.0$ is the photon index. For each value of Γ the spectrum was normalized so that the total energy flux between χ and 200 keV at the surface of the disk was $1 \text{ keV cm}^{-2} \text{ s}^{-1}$. A value of 25 is chosen for the Coulomb logarithm Λ (Brown 1971), but, as seen below, the results are insensitive to its value.

The value of N_{H} and equation (5) determines the upper limit to the outer integral in the numerator of equation (11). $K\alpha$ photons produced by electrons with kinetic energies larger than this are accounted for in a later bin where the column is large enough for the energy of those electrons to pass below χ . Since the largest column we consider is 10^{24}

³ There is a misprint in the expression for G_r in the paper by Hombourger (1998), so the form quoted by Quarles (1976) was used in its place.

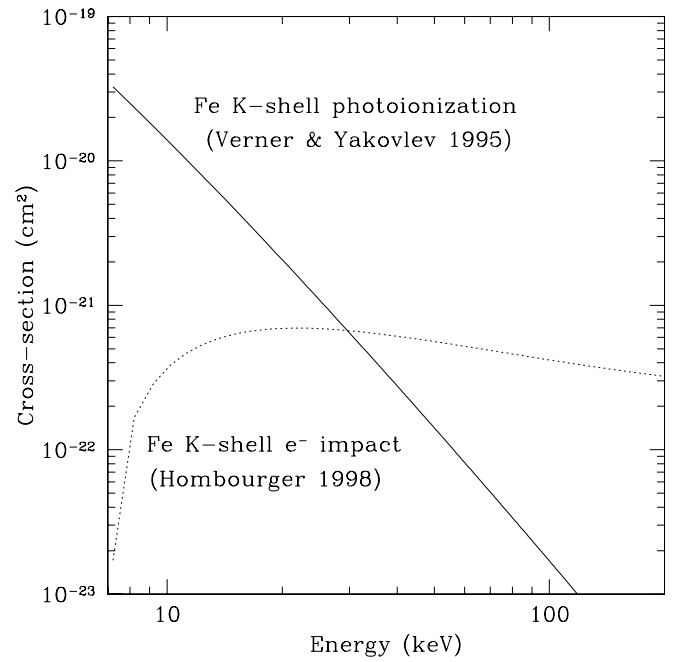


FIG. 1.—K-shell ionization cross section of iron as a function of energy for two different ionization processes. The solid line shows the cross section for photoionization using the fits of Verner & Yakovlev (1995). The dotted line denotes the empirical expression for electron impact cross section found by Hombourger (1998; in this case the x -axis plots electron kinetic energy).

cm^{-2} , there is a slight error as we do not count any Fe $K\alpha$ emission produced by electrons that can pass through this column. However, equation (5) shows that only electrons with kinetic energies greater than $\sim 3.5 \text{ MeV}$ can still ionize iron beyond a column of 10^{24} cm^{-2} . For the electron distributions we consider, there is a negligible amount of electrons with $E > 3.5 \text{ MeV}$, so this slight error will not impact the results.

3.1.1. Power Law \mathcal{N}_E

Modeling of the hard X-ray tails in the GBHCs Cyg X-1 and GRS 1915+105 have shown that the nonthermal electrons responsible for this emission can be described as a soft power law (Gierliński et al. 1999; Zdziarski et al. 2001). Therefore, we first consider electron distributions of the form $\mathcal{N}_E \propto (E/\chi)^{-\gamma}$, where $\gamma = 1, 2, 3, \text{ or } 4$ is the number index. As with the photon distribution, the incident electron power laws are normalized such that the total energy flux between χ and 200 keV is $1 \text{ keV cm}^{-2} \text{ s}^{-1}$. In this way, roughly the same amount of energy is being deposited into the material by both the electrons and photons.

Figure 2 shows the results of computing the ratio $\mathcal{F}_{\text{ei}}/\mathcal{F}_{\text{photo}}$ for the different values of Γ and γ . Each panel shows the results for an individual photon index, while the different lines denote the electron number index. In every case considered here the Fe $K\alpha$ flux from electron impact is a small fraction of that produced by photoionization. The maximum ratio found is $\mathcal{F}_{\text{ei}}/\mathcal{F}_{\text{photo}} \sim 0.01$ when $\Gamma = 1.7$, $\gamma = 1$, and the Thomson depth ($\tau_{\text{T}} = 1.2\sigma_{\text{T}}N_{\text{H}}$) is $\sim 10^{-3}$. The ratio then drops rapidly as the column increases because fewer and fewer electrons are able to penetrate farther into the gas. The only exception is for $\gamma = 1$. This electron spectrum is very flat so that the energy flux per decade

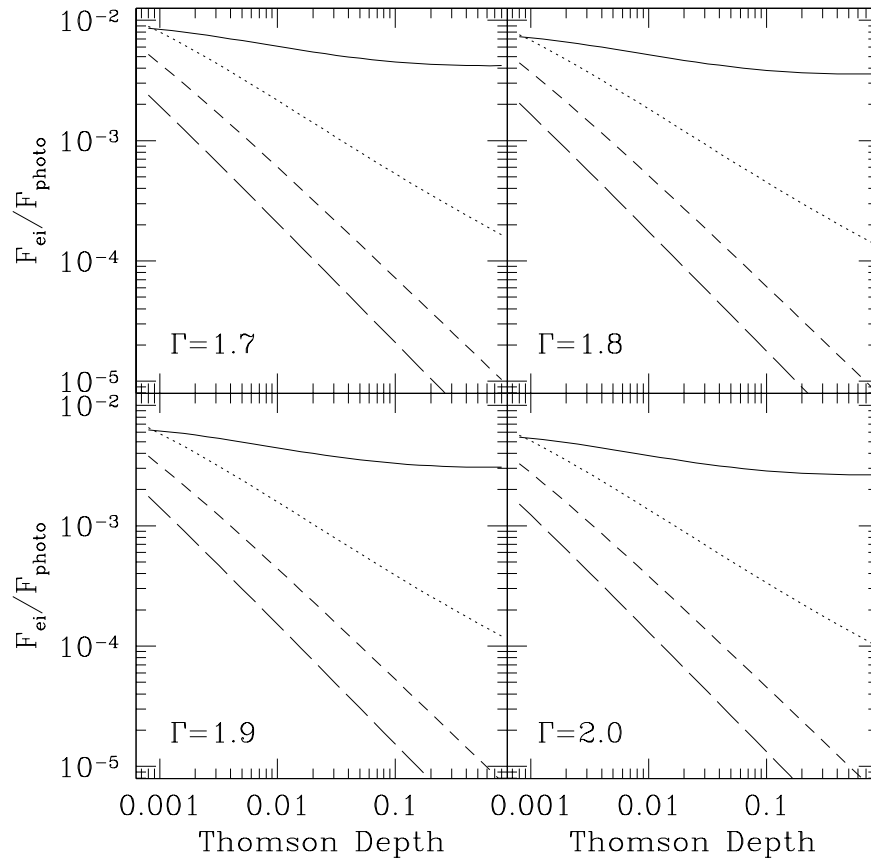


FIG. 2.—Ratio of Fe K α flux from electron impact \mathcal{F}_{ei} to Fe K α flux from photoionization \mathcal{F}_{photo} . Both incident spectra were power laws with the radiation having a photon index Γ and the electrons a number index γ . Both spectra were normalized so that the energy flux between χ and 200 keV was $1 \text{ keV cm}^{-2} \text{ s}^{-1}$. In each panel $\mathcal{F}_{ei}/\mathcal{F}_{photo}$ is plotted for $\gamma = 1$ (solid line), 2 (dotted line), 3 (short-dashed line), and 4 (long-dashed line). In all cases the Fe K α line flux produced by electron impact is negligible compared to the one produced by photoionization.

actually increases with energy, and so there are many high-energy electrons that can still ionize Fe K α at larger column densities. The electron K-shell cross section is close to a constant at high energies (Fig. 1), which helps keep the ratio roughly the same as the column increases. However, even with this extreme spectrum, electron impact is still an inefficient method to produce Fe K α photons.

As γ is increased, the ratio at all τ_T drops. This is a result of the shape of the cross section that peaks at electron energies of ~ 20 keV and not at the ionization threshold, χ (Fig. 1). Therefore, when the electron spectrum softens, more electrons have lower energies below the peak in the cross section, and the Fe K α flux decreases accordingly.

There is also a slight change in $\mathcal{F}_{ei}/\mathcal{F}_{photo}$ with the photon-index. The ratio lowers as Γ increases because for softer photon spectra there are more photons at lower energies, which is where σ_{photo} is larger. This increases the number of K α photons emitted and therefore decreases the ratio.

3.1.2. Thermal \mathcal{N}_E

Observations by *BeppoSAX* have shown that many Seyfert 1 galaxies have high-energy cutoffs between 100 and 300 keV (Matt 2001). If the hard X-rays in these AGNs are produced by thermal Comptonization, then such measurements can constrain the temperature of the coronal electrons by $kT \approx E_c/2$, where E_c is the cutoff energy. We now consider the production of Fe K α photons by electrons in a thermal distribution, described by a Maxwell-Boltzmann distribu-

tion with $kT = 100, 200, 300,$ or 400 keV. As before, the electron spectra were normalized so that the total energy flux incident on the gas between χ and 200 keV was $1 \text{ keV cm}^{-2} \text{ s}^{-1}$, the same as for the photon spectra.

Figure 3 plots the Fe K α flux ratio between electron impact and photoionization for electrons in a thermal distribution. Again, the flux of K α photons produced by the electrons is $\lesssim 1\%$ of that generated by photoionization. An interesting difference between the thermal and power-law electron distributions is that the largest flux ratio occurs some distance into the layer for a Maxwellian population and not at the surface, as was found with the power law. This is because the number of electrons in the thermal distribution peaks at energies $\sim kT$ and can thus ionize Fe to larger columns. Therefore, the maximum ratio moves to greater τ_T for larger kT .

Except for the lowest columns, $\mathcal{F}_{ei}/\mathcal{F}_{photo}$ increases with kT . The total number of electrons in the distribution grows with kT , and, since the spectrum is normalized so that the energy deposited between χ and 200 keV is the same for each case, the excess electrons are found at higher energies. This fact, combined with relative flatness of the K-shell cross section (Fig. 1), explains the small increase in $\mathcal{F}_{ei}/\mathcal{F}_{photo}$ with kT .

3.2. Proton Impact versus Photoionization

We form the ratio of Fe K α flux produced by proton impact to that generated by photoionization by using

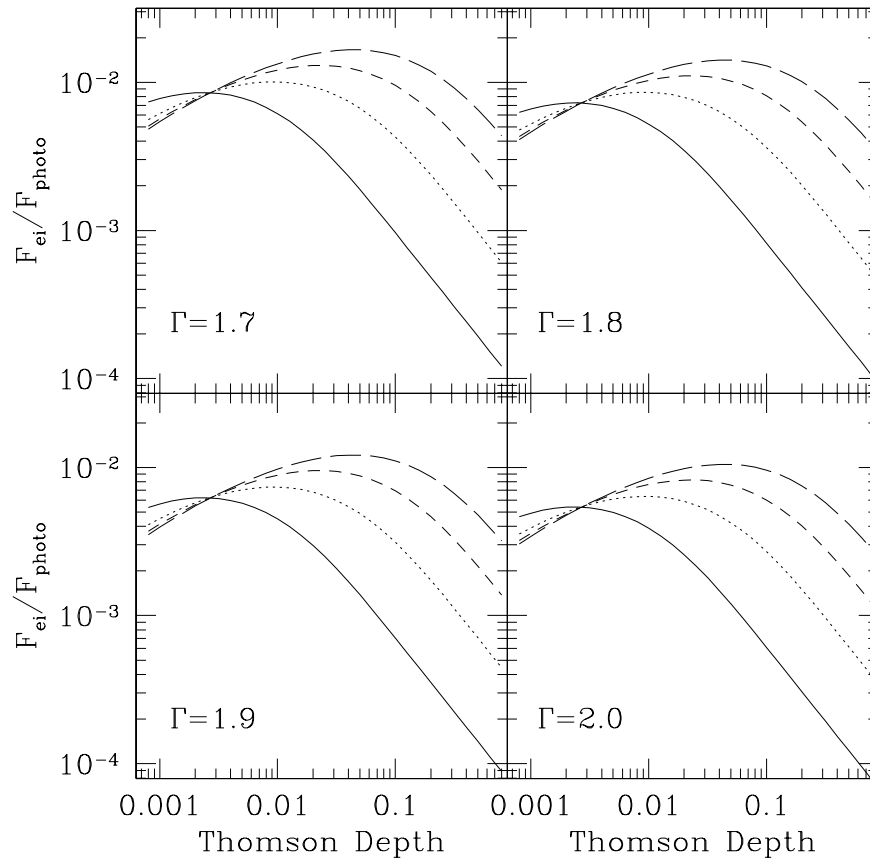


FIG. 3.—Ratio of Fe K α flux from electron impact \mathcal{F}_{ei} to Fe K α flux from photoionization \mathcal{F}_{photo} . The incident radiation spectrum was a power law with a photon index Γ . The incident electron spectrum was a Maxwell-Boltzmann distribution of temperature kT . Both spectra were normalized so that the energy flux between χ and 200 keV was $1 \text{ keV cm}^{-2} \text{ s}^{-1}$. In each panel $\mathcal{F}_{ei}/\mathcal{F}_{photo}$ is plotted for $kT = 100 \text{ keV}$ (solid line), 200 keV (dotted line), 300 keV (short-dashed line), and 400 keV (long-dashed line). In all cases the Fe K α line flux produced by electron impact is negligible compared to the one produced by photoionization.

equations (7) and (10):

$$\frac{\mathcal{F}_{pi}}{\mathcal{F}_{photo}} = \frac{m_e \int_{\chi}^{E_{\min}(N_H)} \mathcal{P}_E(E_0) \left[\int_{\chi}^{E_0} \sigma_{ei}(E) E dE \right] dE_0}{m_p 2\pi e^4 \Lambda N_H \int_{\chi}^{\infty} F_{\epsilon}(\epsilon) \sigma_{photo}(\epsilon) d\epsilon}. \quad (12)$$

The calculation of the denominator of equation (12) is unchanged from the previous section (e.g., $\Lambda = 25$). The K-shell ionization cross section for proton impact was computed by using the empirical formula of Romo-Kröger (1998). This cross section is plotted along with the ones for photoionization and electron bombardment in Figure 4. Unfortunately, the formula is only valid for proton kinetic energies less than $\sim 50 \text{ MeV}$. Through equation (9), this limits the column density that can be probed to be less than $3 \times 10^{23} \text{ cm}^{-2}$.

3.2.1. Thermal \mathcal{P}_E

This section considers the Fe K α flux produced by a distribution of protons at the local virial temperature kT_{vir} . This situation may be applicable to the case where a relatively cold, thin accretion disk overlaps with a hot, ADAF-like flow (Deufel et al. 2002). Because of the 50 MeV cutoff in the proton impact cross section, we are limited to proton spectra that do not have many particles above this energy. A Maxwell-Boltzmann distribution is assumed for the particles, and three cases are considered: $kT = 1.56$, 3.12 , and 6.24 MeV . These values correspond to the virial

temperature at 100 , 50 , and $25 R_S$, respectively. The proton spectra are normalized so that the total energy flux incident on the gas is $1 \text{ keV cm}^{-2} \text{ s}^{-1}$. The Fe K α flux produced by the incident protons will be compared with that from a power-law photon spectrum, which is normalized to $1 \text{ keV cm}^{-2} \text{ s}^{-1}$ between χ and 200 keV .

The results are shown in Figure 5. For each case, it is found that the protons produce a negligible amount of Fe K α emission as compared to photoionization. This is in part due to the normalization conditions. The spectra were normalized so that both the protons and the photons deposited the same amount of energy (per unit area, per unit time) into the material. As the majority of the protons carried 2–3 orders of magnitude more energy than a typical incident photon, there are far fewer protons in the illuminating distribution than photons (this should be contrasted with the situation described in § 3.1, where there was roughly equal numbers of electrons and photons). However, even if the spectra were normalized to the same number flux, the Fe K α emission produced by protons would still be much less than that from photoionization.

Of the three values of kT_{vir} considered, it is the middle one ($kT_{\text{vir}} = 3.12 \text{ MeV}$) that results in the largest $\mathcal{F}_{pi}/\mathcal{F}_{photo}$, owing to the peak in its energy flux residing closest to the maximum cross section (Fig. 4). On the other hand, it is the $kT_{\text{vir}} = 1.56 \text{ MeV}$ spectrum that has the greatest ratio at low τ_T . This is because this distribution has a

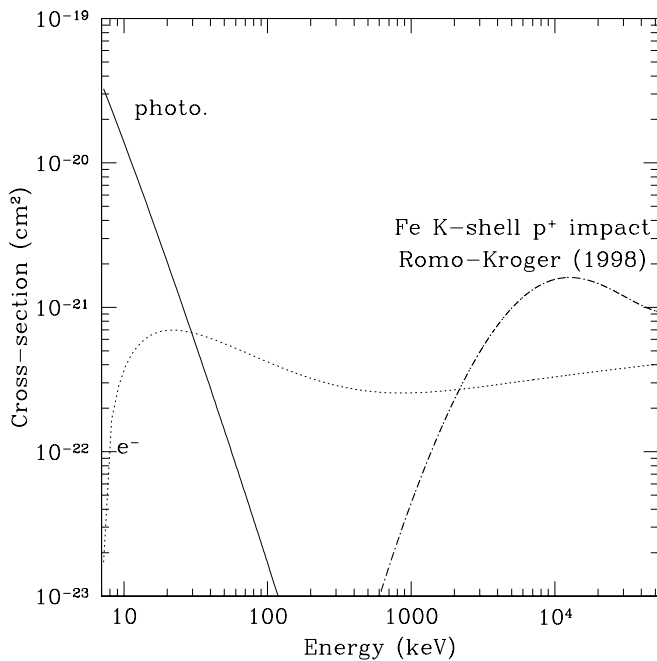


FIG. 4.—Comparison of the Fe K-shell ionization cross section due to proton impact (*dot-dashed line*) with those for electron impact (*dotted line*) and photoionization (*solid line*). The proton impact cross section was taken from the empirical fit of Romo-Króger (1998). This fit is only valid to proton kinetic energies of ~ 50 MeV, so the cross section is truncated at that point.

large number of relatively low energy particles that stop quickly in the gas and thus produce their $K\alpha$ photons close to the surface. The other distributions predominantly have much higher energy particles that can penetrate through to larger columns. One other effect that is noticeable in Figure 5 is the decrease in $\mathcal{F}_{\text{pi}}/\mathcal{F}_{\text{photo}}$ as the photon-index, Γ , increases. As explained in § 3.1.1, the softer photon spectra have more photons at low energies, where the cross section is larger and will produce more $K\alpha$ photons, thereby lowering the ratio.

4. DISCUSSION

We have shown that particle impact is an inefficient method to produce Fe $K\alpha$ emission as compared to photoionization (see also Basko 1979). In this section, we attempt to place this result in the wider context of accretion disk models and particle acceleration mechanisms. We begin with the electron bombardment results and their relation to models of coronae above geometrically thin disks. Proton impact and the two-component disk model is discussed at the end of the section.

4.1. Electrons in Accretion Disk Coronae

It has been argued for some time that the energy responsible for heating the electrons in an accretion disk corona is carried and released by magnetic fields expelled from the disk surface (e.g., Galeev et al. 1979; Di Matteo 1998). The magnetic energy (ultimately derived from the magneto-hydrodynamic [MHD] turbulence in the body of the disk; Miller & Stone 2000) would then be liberated by reconnection events with neighboring field lines, in a deliberate analogy to flares in the lower solar corona. Some fraction of

this energy is deposited into electrons that end up in a thermal distribution. The remaining energy would then be used to accelerate particles (mostly electrons) to high energies. A key parameter is the fraction of energy that is funneled into the nonthermal particles for a given event. Unfortunately, as is discussed below, that number is not well constrained.

X-ray observations have shown that, in the accretion disk environment, the newly energized coronal particles give up their energy to the soft X-ray/UV photons from the accretion disk. This results in the standard hard X-ray Comptonized power law that is the hallmark of these sources. The very hard X-ray tails observed in the spectra of Cyg X-1 and GRS 1915+105 show that the nonthermal particles are involved in this process. The results of § 3.1 have shown that for electrons to be an important contributor to Fe $K\alpha$ production then $\sim 10^2$ – 10^4 times more energy has to be deposited into the disk by particles than by the Comptonized photons. For this scenario to be viable, most of the electrons in the corona would have to not lose their energy to Comptonization, implying a very low Compton y -parameter. However, the observed photon indices and high-energy cutoffs show that $y \sim 1$ in most of these systems (Petrucci et al. 2001); therefore, Comptonization is important. Alternatively, owing to outflows in the corona, the hard X-rays may be beamed away from the disk resulting in a very small radiation flux on the surface (Beloborodov 1999). This scenario is also unlikely, as particles would have to be both outflowing (to beam the hard X-rays away from the disk) and streaming toward the disk to generate the Fe $K\alpha$ line. Furthermore, the Compton reflection hump seen in many Seyfert 1 galaxies shows that roughly half the observed X-ray flux must be intercepted by optically thick material. Perhaps a more fundamental problem with a very strong particle flux on the disk surface is that $\gg 99\%$ of the incident energy goes into heat and not radiation (Tatischeff 2002). This would lead to a strong expansion of the surface layers and perhaps lead to evaporation, as is envisaged in the proton-illuminated disks (Deufel et al. 2002), which would certainly affect the observed optically thick signatures such as the Compton reflection bump.

On the other hand, the nonthermal particles are likely to be tied to the magnetic field lines in the corona. Thus, there may be a large particle flux at the position of the magnetic footpoints on the surface of the accretion disk. In these very local positions, the electron flux may be much higher than the radiation flux, and Fe $K\alpha$ may be dominated by the electron impact process. Indeed, such bright spots are seen on the surface of the Sun as sources of hard X-rays (Hudson et al. 1994; Kundu et al. 1995). However, such small regions are unlikely to be detected amidst the unresolved accretion disk emission.

The dominance of the Comptonized hard X-ray power law in the spectra of accreting black holes implies that the acceleration of nonthermal particles in the corona is not highly efficient. This conclusion is supported by the above results on Fe $K\alpha$ production by electron impact.⁴ The mechanism by which electrons are accelerated to large kinetic energies in accretion disk coronae is not known.

⁴ Analogous arguments can be made against conduction from the corona as an important heat source for the disk (e.g., Rózańska 1999; Rózańska & Czerny 2000b). In a magnetically dominated corona, the electrons are more likely to be Compton-cooled before conduction can be effective.

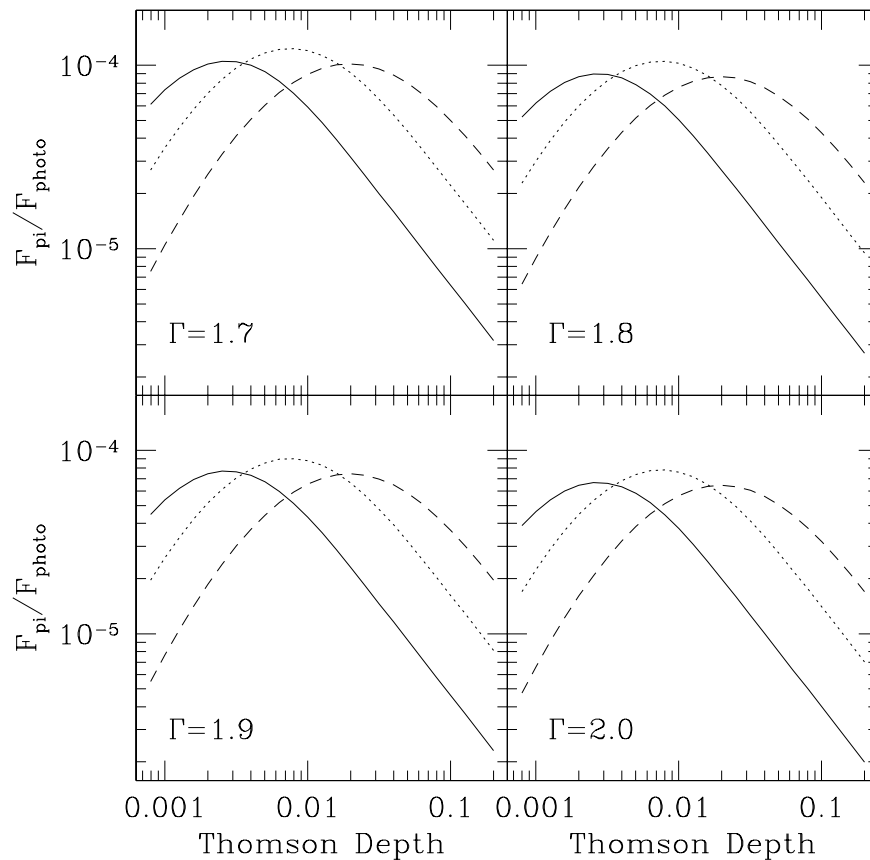


FIG. 5.—Ratio of Fe K α flux from proton impact \mathcal{F}_{pi} to Fe K α flux from photoionization $\mathcal{F}_{\text{photo}}$. The incident radiation spectrum was a power law with a photon index Γ . The incident proton spectrum was a Maxwell-Boltzmann distribution of temperature kT . The radiation spectrum was normalized so that the energy flux between χ and 200 keV was $1 \text{ keV cm}^{-2} \text{ s}^{-1}$. The proton spectrum was normalized so that the total energy flux was $1 \text{ keV cm}^{-2} \text{ s}^{-1}$. In each panel $\mathcal{F}_{\text{pi}}/\mathcal{F}_{\text{photo}}$ is plotted for $kT = 1.56 \text{ MeV}$ (solid line) corresponding to the virial temperature at $100 R_S$, 3.12 MeV (dotted line, $50 R_S$), and 6.24 MeV (short-dashed line, $25 R_S$). In all cases the Fe K α line flux produced by proton impact is negligible compared to the one produced by photoionization. The cutoff in the proton ionization cross section (see Fig. 4) limits the calculations to low Thomson depth and low virial temperatures.

Again, one can look to the solar corona for guidance, where there are three different processes that are considered to be viable candidates (see Miller et al. 1997 and Miller 1998 for recent reviews). The first is stochastic acceleration by MHD waves in the coronal plasma that are excited by the reconnection events. The second is shock acceleration by the plasma jets produced by reconnection (e.g., Blackman & Field 1994). However, it is thought that the shocks are unlikely to be strong enough to account for most energetic particles (that is, shocks may only “pre-accelerate”), although they may provide the bulk of the heat that goes into the thermal electrons (Di Matteo 1998). The third process is direct acceleration by large-scale electric fields, such as those found in reconnecting current sheets. The efficiency of all of these processes is, at this point, largely unknown, but numerical reconnection simulations are beginning to show that electric field acceleration may be $\lesssim 10\%$ efficient (Nodes et al. 2003).

Before leaving the discussion of nonthermal electrons, we can use some of the basic analytical results of electric field acceleration as a consistency check of our conclusions. When thermal electrons are subjected to an external electric field they will begin to accelerate along the direction of the field, but for most of the particles, this motion will be limited by Compton drag. However, the collisional drag force on electrons decreases with the velocity, so that particles with a

large enough speed can “run away” and be accelerated freely by the electric field. The value of the electric field where this critical runaway velocity is equal to the thermal velocity v_e of a Maxwellian distribution is called the Dreicer field and is given by (Dreicer 1959, 1960)

$$\mathcal{E}_D = e \left(\frac{\omega_e}{v_e} \right)^2 \Lambda, \quad (13)$$

where ω_e is the electron plasma frequency. In this situation, the bulk of the electrons in the thermal distribution will be accelerated.

In the context of solar flares, Holman (1985) examined the properties of accelerated electrons by sub-Dreicer electric fields.⁵ Since the magnetic field induced by the electron beam must be less than the field in the acceleration region (B), Holman (1985) found that this limited the acceleration rate (per area) to a maximum of $cB/2\pi eL$, where L is the length of the accelerating current sheet (see also Holman, Kundu, & Kane 1989). If the radiation flux on the disk is $10^{15} \text{ ergs cm}^{-2} \text{ s}^{-1}$ between 10 eV and 100 keV (Ross,

⁵ Super-Dreicer acceleration has been considered by, e.g., Litvinenko (1996) and Craig & Litvinenko (2002), where the acceleration of the electrons are limited by transverse magnetic fields.

Fabian, & Young 1999; Ballantyne, Ross, & Fabian 2001), then for a $\Gamma = 1.9$ spectrum, this translates to $\sim 10^{20}$ ergs $\text{cm}^{-2} \text{s}^{-1}$ between χ and 200 keV. For a significant Fe K α flux due to electron impact, the energy flux due to electrons must be $\sim 10^{23}$ ergs $\text{cm}^{-2} \text{s}^{-1}$ (Fig. 2). Converting this to a number flux using a $\gamma = 3$ spectrum, and plugging into the acceleration limit above gives an estimate of the accelerating magnetic field in the accretion disk coronae, $B \sim (10^{11} L) \text{ G}$. For comparison, the equipartition magnetic field in a disk is $\sim 10^8 \text{ G}$ (Merloni & Fabian 2001). Thus, the assumptions of sub-Dreicer acceleration of nonthermal particles and significant Fe K α emission from electron impact implies an extremely strong coronal magnetic field.

4.2. Protons and Truncated Accretion Disks

Considerable work over the last few years has been done investigating the properties of disks that change from being cold and geometrically thin to hot and geometrically thick (see references in § 1). One of the greatest difficulties in describing such a model is the process by which the truncation of the cold disk occurs. A natural mechanism would be heating the disk until its local scale height becomes comparable to the radius, effectively evaporating the inner part of the disk.

Once the two-phase accretion flow is operating, Deufel et al. (2002) showed that protons in the hot phase striking the cold disk will be an effective mechanism for heating the disk surface. Comptonization of the soft disk photons by this heated layer produced a hard X-ray spectrum not too dissimilar from what is observed. In § 3.2 we found that virialized protons are a highly inefficient way of producing Fe K α emission. Thus, external hard X-ray radiation will need to be included in the models of truncated accretion flows to explain any Fe K emission. In the context of the proton illumination model, it may be possible to determine the relative importance of radiation heating to proton heating by examining the equivalent width of the Fe K α line.

4.3. Other Applications

The preceding sections have shown that it is difficult for particle impact to be an efficient producer of Fe K α lines, because most of the incoming energy is used to heat the gas and not for ionizing iron. Thus, this process will only be important in environments where photons are not as efficiently produced as high-energy particles. While detailed calculations are beyond the scope of this paper, nonthermal

radio sources or jetlike flows, where the bulk of the energy may be transported by relativistic particles, may be areas where particle impact is the dominant source of ionization. The shock front in a gamma-ray burst is another possible area of application if there are enough high-energy baryons in the relativistic outflow.

5. SUMMARY

Just like a photon, high-energy electrons and protons can eject a K-shell electron from iron and produce a K α line photon if their kinetic energy is greater than 7.112 keV. In this paper we have considered the possible role of particle impact in the generation of Fe K α emission from accreting black holes. Calculations of Fe K α flux from various columns of gas were performed when it was bombarded by a nonthermal power law of electrons, or a thermal distribution of electrons or protons. This flux was then compared with that produced by a power law of radiation under the assumption that all process deposited roughly 1 erg $\text{cm}^{-2} \text{s}^{-1}$ of energy into the material. It was found that in every circumstance the Fe K α flux produced by particle impact was less than 1% of that produced by photoionization. A more realistic calculation that relaxes the optically thin assumption made here would find an even smaller ratio.

Increasing the electron flux on the accretion disk in order to produce more K α emission was inconsistent with the standard disk-corona model for accretion disk emission. In the case of a disk illuminated by virialized protons, as might be found in a truncated accretion disk model, we found a very low efficiency for Fe K α production. Therefore, these type of models must consider external X-ray illumination to explain any observed K α line.

To conclude, we find that, except for isolated regions around magnetic footpoints, it is unlikely that particle impact can significantly contribute to the observed X-ray line (or continuum) emission from accreting black holes. Depending on the efficiency of the unknown acceleration mechanisms, particles may, however, be an important heating source for accretion disks.

D. R. B. was supported by the Natural Sciences and Engineering Research Council of Canada. A. C. F. thanks the Royal Society for support. We thank the anonymous referee for useful comments.

APPENDIX

UNNORMALIZED LINE FLUXES FROM PARTICLE IMPACT

In the interests of generality, we show in Figure 6 the unnormalized Fe K α line fluxes (in photons $\text{cm}^{-2} \text{s}^{-1}$) obtained from equations (4) and (7) for the power law and thermal spectral shapes used in § 3. The standard values of $\omega = 0.342$ and $\beta = 0.822$ from Bambynek et al. (1972) were used, and the solar Fe abundance of $A_{\text{Fe}} = 2.82 \times 10^{-5}$ from Holweger (2001) was assumed. As the Fe abundance is just a multiplicative factor, the results can be easily scaled to other metallicities. Finally, the particle spectra were normalized as in § 3; that is, the electron spectra has a energy flux between 7.112 and 200 keV of 1 keV $\text{cm}^{-2} \text{s}^{-1}$, while the protons have a total energy flux of 1 keV $\text{cm}^{-2} \text{s}^{-1}$. Again, the results in Figure 6 can be easily scaled to other impacting fluxes.

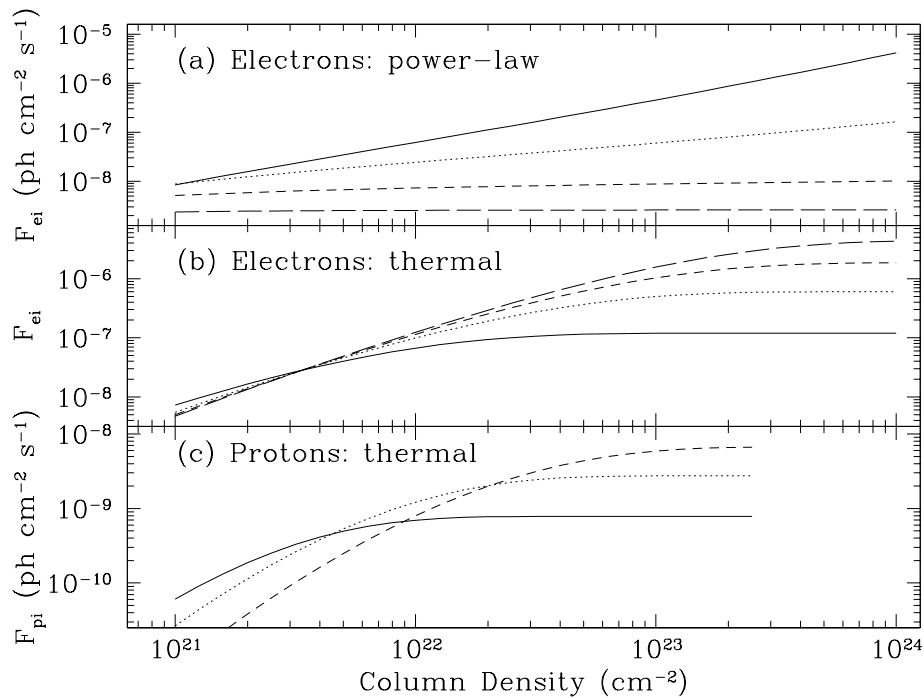


FIG. 6.—Iron $K\alpha$ flux in photons $\text{cm}^{-2} \text{s}^{-1}$ produced by particle impact as a function of hydrogen column density. A solar abundance of iron has been assumed. (a) Line flux produced by electron impact when the particles have a power-law spectrum. The energy flux between 7.112 and 200 keV was $1 \text{ keV cm}^{-2} \text{ s}^{-1}$. The line styles are the same as in Fig. 2. (b) Line flux produced by electron impact when the particles have a thermal spectrum. The energy flux between 7.112 and 200 keV was $1 \text{ keV cm}^{-2} \text{ s}^{-1}$. The line styles are the same as in Fig. 3. (c) Line flux produced by proton impact when the particles have a thermal spectrum. The total energy flux was $1 \text{ keV cm}^{-2} \text{ s}^{-1}$. The line styles are the same as in Fig. 5, and the 50 MeV cutoff in the proton ionization cross section limited the calculation to lower column densities.

REFERENCES

- Bai, T. 1979, *Sol. Phys.*, 62, 113
 Ballantyne, D. R., Ross, R. R., & Fabian, A. C. 2001, *MNRAS*, 327, 10
 Ballantyne, D. R., Vaughan, S., & Fabian, A. C. 2003, *MNRAS*, in press
 Bambynek, W., Craseman, B., Fink, R. W., Freund, H. U., Mark, H., Swift, C. D., Price, R. E., & Rao, P. V. 1972, *Rev. Mod. Phys.*, 44, 716
 Barrio, F. E., Done, C., & Nayakshin, S. 2003, *MNRAS*, in press
 Basko, M. M. 1978, *ApJ*, 223, 268
 ———. 1979, *AZh*, 56, 399 (*Sov. Astron.*, 23, 224)
 Beloborodov, A. M. 1999, *ApJ*, 510, L123
 Blackman, E. G., & Field, G. B. 1994, *Phys. Rev. Lett.*, 73, 3097
 Brown, J. C. 1971, *Sol. Phys.*, 18, 489
 Chiang, J., Reynolds, C. S., Blaes, O. M., Nowak, M. A., Murray, N., Madajski, G., Marshall, H. L., & Magdziarz, P. 2000, *ApJ*, 528, 292
 Coppi, P. S. 1999, in *ASP Conf. Proc.* 161, *High-Energy Processes in Accreting Black Holes*, ed. J. Poutanen & R. Svensson (San Francisco: ASP), 375
 Craig, I. J. D., & Litvinenko, Y. E. 2002, *ApJ*, 570, 387
 Dennis, B. R., & Schwartz, R. A. 1989, *Sol. Phys.*, 121, 75
 Deufel, B., Dullemond, C. P., & Spruit, H. C. 2002, *A&A*, 387, 907
 Deufel, B., & Spruit, H. C. 2000, *A&A*, 362, 1
 Di Matteo, T. 1998, *MNRAS*, 299, L15
 Di Matteo, T., Blackman, E. G., & Fabian, A. C. 1997, *MNRAS*, 291, L23
 Done, C., & Zycki, P. T. 1999, *MNRAS*, 305, 457
 Dreicer, H. 1959, *Phys. Rev.*, 115, 238
 ———. 1960, *Phys. Rev.*, 117, 329
 Emslie, A. G. 1978, *ApJ*, 224, 241
 Emslie, A. G., Phillips, K. J. H., & Dennis, B. R. 1986, *Sol. Phys.*, 103, 89
 Esin, A. A., McClintock, J. E., & Narayan, R. 1997, *ApJ*, 489, 865
 Fabian, A. C., Iwasawa, K., Reynolds, C. S., & Young, A. J. 2000, *PASP*, 112, 1145
 Fabian, A. C., & Vaughan, S. 2003, *MNRAS*, 340, L28
 Fabian, A. C., et al. 2002, *MNRAS*, 335, L1
 Galeev, A. A., Rosner, R., & Vaiana, G. S. 1979, *ApJ*, 229, 318
 George, I. M., & Fabian, A. C. 1991, *MNRAS*, 249, 352
 Ghisellini, G., Haardt, F., & Matt, G. 1994, *MNRAS*, 267, 743
 Gierliński, M., Zdziarski, A. A., Poutanen, J., Coppi, P. S., Ebisawa, K., & Johnson, W. N. 1999, *MNRAS*, 309, 496
 Guilbert, P. W., & Rees, M. J. 1988, *MNRAS*, 233, 475
 Haardt, F., & Maraschi, L. 1991, *ApJ*, 380, L51
 ———. 1993, *ApJ*, 413, 507
 Haardt, F., Maraschi, L., & Ghisellini, G. 1994, *ApJ*, 432, L95
 Hatchett, S., & Weaver, R. 1977, *ApJ*, 215, 285
 Holman, G. D. 1985, *ApJ*, 293, 584
 Holman, G. D., Kundu, M. R., & Kane, S. R. 1989, *ApJ*, 345, 1050
 Holweger, H. 2001, in *AIP Conf. Vol. 598. Joint SOHO/ACE Workshop Solar and Galactic Composition*, ed. R. F. Wimmer-Schweingruber (New York: AIP), 23
 Hombourger, C. 1998, *J. Phys. B*, 31, 3693
 Hudson, H. S., Strong, K. T., Dennis, B. R., Zarro, D., Inda, M., Kosugi, T., & Sakao, T. 1994, *ApJ*, 422, L25
 Ichimaru, S. 1977, *ApJ*, 214, 840
 Krolik, J. H., Madau, P., & Życki, P. T. 1994, *ApJ*, 420, L57
 Kundu, M. R., Nitta, N., White, S. M., Shibasaki, K., Enome, S., Sakao, T., Kosugi, T., & Sakurai, T. 1995, *ApJ*, 454, 522
 Lightman, A. P., & White, T. R. 1988, *ApJ*, 335, 57
 Litvinenko, Y. E. 1996, *ApJ*, 462, 997
 Manmoto, T., & Kato, S. 2000, *ApJ*, 538, 295
 Manmoto, T., Kato, S., Nakamura, K. E., & Narayan, R. 2000, *ApJ*, 529, 127
 Martocchia, A., Matt, G., Karas, V., Belloni, T., & Feroci, M. 2002, *A&A*, 387, 215
 Matt, G. 2001, in *AIP Conf. Proc. 599, X-Ray Astronomy: Stellar End-points, AGN, and the Diffuse X-Ray Background*, ed. N. E. White, G. Magaluti, & G. Palumbo (New York: AIP), 209
 Matt, G., Perola, G. C., & Piro, L. 1991, *A&A*, 247, 25
 Merloni, A., & Fabian, A. C. 2001, *MNRAS*, 321, 549
 Meyer, F., & Meyer-Hofmeister, E. 1994, *A&A*, 288, 175
 Meyer, F., Liu, B. F., & Meyer-Hofmeister, E. 2000, *A&A*, 361, 175
 Miller, J. A. 1998, *Space Sci. Rev.*, 86, 79
 Miller, J. A., et al. 1997, *J. Geophys. Res.*, 102, 14631
 Miller, J. M., et al. 2002a, *ApJ*, 570, L69
 ———. 2002b, *ApJ*, 577, L15
 ———. 2002c, *ApJ*, 578, 348
 Miller, K. A., & Stone, J. M. 2000, *ApJ*, 534, 398
 Mushotzky, R. F., Done, C., & Pounds, K. A. 1993, *ARA&A*, 31, 717
 Nandra, K., George, I. M., Mushotzky, R. F., Turner, T. J., & Yaqoob, T. 1997, *ApJ*, 477, 602
 ———. 1999, *ApJ*, 523, L17
 Nandra, K., & Pounds, K. A. 1994, *MNRAS*, 268, 405
 Narayan, R., & Yi, I. 1994, *ApJ*, 428, L13
 Nöcker, C., Birk, G. T., Lesch, H., & Schopper, R. 2003, *Plasma Phys.*, 10, 835
 Petrucci, P. O., et al. 2001, *ApJ*, 556, 716
 ———. 2002, *A&A*, 388, L5
 Pounds, K. A., Nandra, K., Stewart, G. C., George, I. M., & Fabian, A. C. 1990, *Nature*, 344, 132

- Quarles, C. A. 1976, *Phys. Rev. A*, 13, 1278
- Quataert, E., Di Matteo, T., Narayan, R., & Ho, L. C. 1999, *ApJ*, 525, L89
- Rees, M. J., Begelman, M. C., Blandford, R. D., & Phinney, E. S. 1982, *Nature*, 295, 17
- Reeves, J. N., & Turner, M. J. L. 2000, *MNRAS*, 316, 234
- Reynolds, C. S. 2000, *ApJ*, 533, 811
- . 2001, in *ASP Conf. Ser. 24, Probing the Physics of Active Galactic Nuclei by Multiwavelength Monitoring*, ed. B. A. Peterson, R. S. Polidan, & R. W. Pogge (San Francisco: ASP), 105
- Reynolds, C. S., & Nowak, M. A. 2003, *Phys. Rep.*, 377, 389
- Romo-Kröger, C. M. 1998, *Nucl. Instrum. Methods Phys. Res. B*, 136, 196
- Ross, R. R., Fabian, A. C., & Young, A. J. 1999, *MNRAS*, 306, 461
- Rózańska, A. 1999, *MNRAS*, 308, 751
- Rózańska, A., & Czerny, B. 2000a, *A&A*, 360, 1170
- . 2000b, *MNRAS*, 316, 473
- Shapiro, S. L., Lightman, A. P., & Eardley, D. M. 1976, *ApJ*, 204, 187
- Spitzer, L. 1962, *Physics of Fully Ionized Gases* (2d ed.; New York: Interscience)
- Spruit, H., & Deufel, B. 2002, *A&A*, 387, 918
- Spruit, H. C., & Haardt, F. 2000, *MNRAS*, 315, 751
- Tanaka, Y. 2002, *A&A*, 382, 1052
- Tanaka, Y., Miyaji, T., & Hasinger, G. 1999, *Astron. Nachr.*, 320, 181
- Tanaka, Y., et al. 1995, *Nature*, 375, 659
- Tatischeff, V. 2002, preprint (astro-ph/0208397)
- Vaughan, S., & Edelson, R. 2001, *ApJ*, 548, 694
- Verner, D. A., & Yakovlev, D. G. 1995, *A&AS*, 109, 125
- Zarro, D. M., Dennis, B. R., & Slater, G. L. 1992, *ApJ*, 391, 865
- Zdziarski, A. A., Grove, J. E., Poutanen, J., Rao, A. R., & Vadawale, S. V. 2001, *ApJ*, 554, L45